

Supporting Information for
Heterometallic Strategy to Achieve Large Magnetocaloric Effect
in Polymeric 3d Complexes

Jiong-Peng Zhao,^{a,b} Song-De Han,^a Xue Jiang,^a Sui-Jun Liu,^a Ran Zhao,^a Ze Chang^a and Xian-He Bu^{*a}

^a*TKL of Metal- and Molecule-Based Material Chemistry, and Collaborative Innovation Center of Chemical Science and Engineering (Tianjin), Nankai University, Tianjin 300071, P.R. China.*

^b*School of Chemistry and Chemical Engineering, Tianjin University of Technology, Tianjin 300384, P.R. China.*

* Corresponding author. Fax: (+86) 22-23502458. E-mail: buxh@nankai.edu.cn

Experimental Section

Materials and methods. All chemicals were reagent grade and used as purchased without further purification. Elemental analyses (C, H, and N) were performed on a Perkin-Elmer 240C analyzer (Perkin-Elmer, USA). The XRPD spectra were recorded on a Rigaku D/Max-2500 diffractometer at 40 kV, 100 mA for a Cu-target tube and a graphite monochromator. Simulation of the XRPD spectrum was carried out by the single-crystal data and diffraction-crystal module of the Mercury (Hg) program available free of charge *via* the internet at <http://www.iucr.org>. IR spectra were measured in the range of 400-4000 cm⁻¹ on a Tensor 27 OPUS FT-IR spectrometer using KBr pellets (Bruker, German). Magnetic susceptibility was measured by a Quantum Design MPMS superconducting quantum interference device (SQUID). Diamagnetic corrections were estimated by using Pascal constants and background corrections by experimental measurement on sample holders.

X-ray Crystallography. The single-crystal X-ray diffraction data of **1**, **2** and **4** were collected on a Rigaku SCX-mini diffractometer at 293(2) K, but **3** on a Rigaku 007 Saturn 70 diffractometer at 113(2) K, with Mo-K α radiation ($\lambda = 0.71073 \text{ \AA}$) by ω scan mode. The program *CrystalClear^{SI}* was used for the integration of the diffraction profiles. The structure was solved by direct method using the SHELXS program of the SHELXTL package and refined by full-matrix least-squares methods with SHELXL (semi-empirical absorption corrections were applied by using the SADABS program).^{S2} The non-hydrogen atoms were located in successive difference Fourier syntheses and refined with anisotropic

thermal parameters on F^2 . All hydrogen atoms of were generated theoretically at the specific atoms and refined isotropically with fixed thermal factors. The selected bond lengths and angles are given in Tables S1.

References

S1. G. M. Sheldrick, *SHELXL97, Program for Crystal Structure Refinement*; University of Göttingen: Göttingen, Germany, 1997.

S2. CrystalClear and CrystalStructure; Rigaku/MSC: The Woodlands, TX, 2005.

Elemental analysis (%) calcd for **1**, $C_8H_{14}CrMnNO_{12}$ (423.14): C 22.71, H 3.33, N 3.31%; found for **1**: C 22.35, H 3.61, N 3.69%; calcd for **2**, $C_7H_{12}CrMnNO_{12}$ (409.10): C 20.55, H 2.96, N 3.42%; found for **2**: C 20.74, H 3.17, N 3.76%; calcd for **3**, $C_8H_{14}AlMnNO_{12}$ (398.12): C 24.14, H 3.54, N 3.52%; found for **3**: C 24.47, H 3.25, N 3.84%; calcd for **4**, $C_8H_{14}CrMgNO_{12}$ (392.50): C 24.48, H 3.60, N 3.57%; found for **3**: C 24.64, H 3.92, N 3.96%.

IR (KBr) for **1**: 3173(m), 2883(w), 1599(s), 1453(s), 1388(s), 1346(s), 1084(w), 1014(w), 883(w), 828(s), 428(s); for **2**: 3160(m), 2886(w), 1593(s), 1388(s), 1347(s), 1065(s), 968(w), 942(w), 884(w), 830(s), 430(s); for **3**: 3157 (s), 2892(w), 1620(s), 1455(W), 1397(s), 1365(s), 1124(m), 1015(m), 834(s), 605(w), 472(s); for **4**: 3161(m), 2893(w), 1614(s), 1453(m), 1397(s), 1347(s), 1138(m), 1014(w), 832(s), 436(s).

Table S1. Selected bond lengths [Å] for **1 - 4**.

	1	2	3	4
Mn1—O2 ⁱ	2.1728 (15)	Mn1—O2 ⁱ	2.179 (2)	Mn1—O2 ⁱ 2.1533 (16) Mg1—O2 ⁱ 2.060 (2)
Mn1—O2 ⁱⁱ	2.1728 (15)	Mn1—O2 ⁱⁱ	2.179 (2)	Mn1—O2 ⁱⁱ 2.1533 (16) Mg1—O2 ⁱⁱ 2.060 (2)
Mn1—O2 ⁱⁱⁱ	2.1728 (15)	Mn1—O2 ⁱⁱⁱ	2.179 (2)	Mn1—O2 ⁱⁱⁱ 2.1533 (16) Mg1—O2 ⁱⁱⁱ 2.060 (2)
Mn1—O2 ^{iv}	2.1728 (15)	Mn1—O2 ^{iv}	2.179 (2)	Mn1—O2 ^{iv} 2.1533 (16) Mg1—O2 ^{iv} 2.060 (2)
Mn1—O2	2.1728 (15)	Mn1—O2 ^v	2.179 (2)	Mn1—O2 ^v 2.1533 (16) Mg1—O2 2.060 (2)
Mn1—O2 ^v	2.1728 (15)	Mn1—O2	2.179 (2)	Mn1—O2 2.1533 (16) Mg1—O2 2.060 (2)
Cr1—O1 ^{vi}	1.9782 (13)	Cr1—O1 ^{vi}	1.983 (2)	Al1—O1 ^{vi} 1.9022 (14) Cr1—O1 ^{vi} 1.973 (2)
Cr1—O1	1.9782 (13)	Cr1—O1	1.983 (2)	Al1—O1 1.9022 (14) Cr1—O1 1.973 (2)
Cr1—O1 ^{vii}	1.9782 (13)	Cr1—O1 ^{vii}	1.983 (2)	Al1—O1 ^{vii} 1.9022 (14) Cr1—O1 ^{vii} 1.973 (2)
Cr1—O1 ^{viii}	1.9782 (13)	Cr1—O1 ^{viii}	1.983 (2)	Al1—O1 ^{viii} 1.9022 (14) Cr1—O1 ^{viii} 1.973 (2)
Cr1—O1 ^{ix}	1.9782 (13)	Cr1—O1 ^{ix}	1.983 (2)	Al1—O1 ^{ix} 1.9022 (14) Cr1—O1 ^{ix} 1.973 (2)
Cr1—O1 ^x	1.9782 (13)	Cr1—O1 ^x	1.983 (2)	Al1—O1 ^x 1.9022 (14) Cr1—O1 ^x 1.973 (2)

Symmetry Code: ⁱ $x, x-y+1, -z+1/2$; ⁱⁱ $-x+y, -x+1, z$; ⁱⁱⁱ $-x+y, y, -z+1/2$; ^{iv} $-y+1, x-y+1, z$;

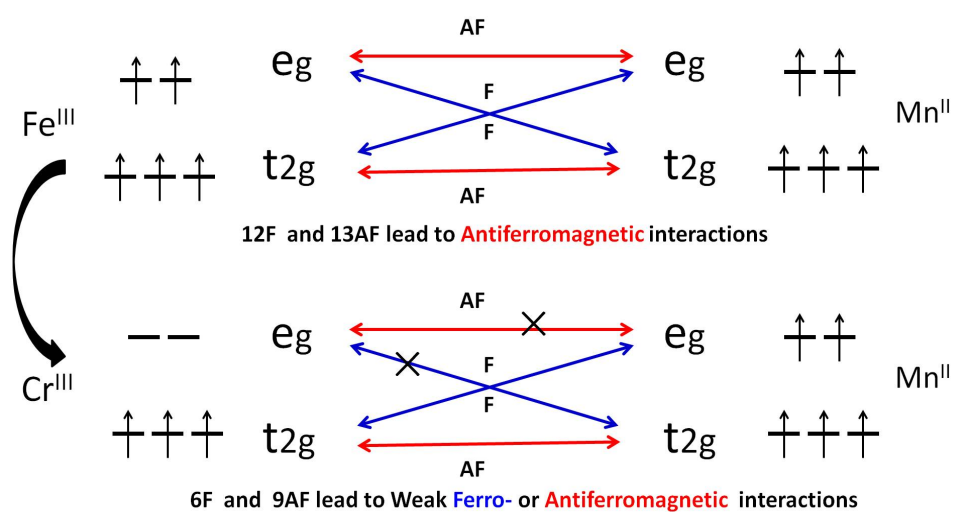
^v $-y+1, -x+1, -z+1/2$; ^{vi} $-x, -y, -z$; ^{vii} $y, -x+y, -z$; ^{viii} $-y, x-y, z$; ^{ix} $x-y, x, -z$; ^x $-x+y, -x, z$.

Table S2. Comparison of $-\Delta S_m$ among our complexes (**1** and **2**) and some reported ones with the $-\Delta S_m$ value above $36.0 \text{ J kg}^{-1} \text{ K}^{-1}$ ($\Delta H = 7 \text{ T}$).

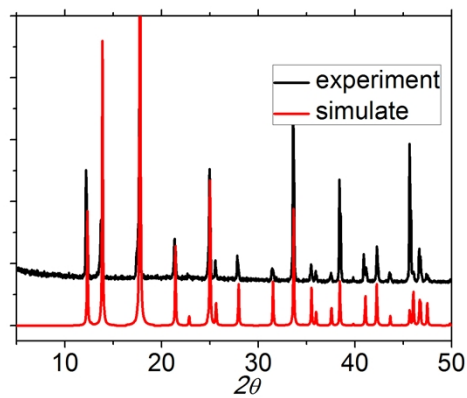
Complexes	Dimensionality	Types of metal ions	$-\Delta S_m/\text{JKg}^{-1}\text{K}^{-1}$ ($\Delta H=7\text{T}$)	Refs
[Mn(glc) ₂ (H ₂ O) ₂]	0D	3d	60.3	1
Gd(HCO ₂) ₃	3D	4f	55.9	2
[Mn(H ₂ O) ₆][MnGd(oda) ₃] ₂ ·6H ₂ O	3D	3d-4f	50.1	3
Complex 2	3D	3d-3d	48.2	this work
[Gd ₆ (OH) ₈ (suc) ₅ (H ₂ O) ₂] _n	3D	4f	48.0	10
[Gd ₂ (OAc) ₃ (H ₂ O) _{0.5}] _n	1D	4f	47.7	4
[Gd(C ₄ O ₄)(OH)(H ₂ O) ₄] _n	3D	4f	47.3	12
Gd(HCOO)(bdc) _n	3D	4f	47.0	11
[Gd ₆ O(OH) ₈] _n	3D	4f	46.6	13
[Gd ₂₄ (DMC) ₃₆ (μ ₄ -CO ₃) ₁₈ (μ ₃ -H ₂ O) ₂] _n ·6H ₂ O	0D	4f	46.1	5
[Gd(HCOO)(OAc) ₂ (H ₂ O) ₂] _n	2D	4f	45.9	6
[Gd ₂ (OAc) ₃ (MeOH)] _n	1D	4f	45.0	4
Complex 1	3D	3d-3d	43.93	this work
[Gd ₂ (OAc) ₆ (H ₂ O) ₄] _n ·4H ₂ O	0D	4f	41.6	7
{Co ₁₀ Gd ₄₂ }	0D	3d-4f	41.26	8
{Ni ₁₀ Gd ₄₂ }	0D	3d-4f	38.2	9
[Gd ₄ (OAc) ₄ (acac) ₈ (H ₂ O) ₄]	0D	4f	37.7	4
{Ni ₁₂ Gd ₃₆ }	0D	3d-4f	36.3	9

References:

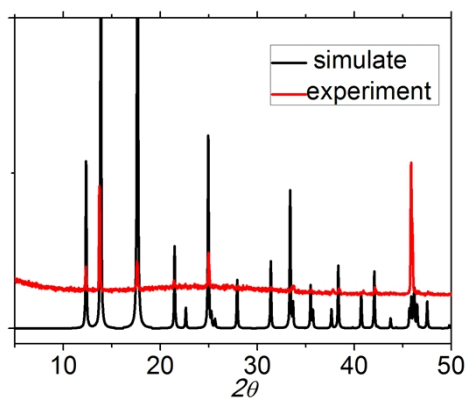
1. Y.-C. Chen, F.-S. Guo, J.-L. Liu, J.-D. Leng, P. Vrabel, M. Orendac, J. Prokleška, V. Sechovský and M.-L. Tong, *Chem. Eur. J.*, 2014, **20**, 3029.
2. G. Lorusso, J. W. Sharples, E. Palacios, O. Roubeau, E. K. Brechin, R. Sessoli, A. Rossin, F. Tuna, E. J. L. McInnes, D. Collison and M. Evangelisti, *Adv. Mater.*, 2013, **25**, 4653
3. F. S. Guo, Y. C. Chen, J. L. Liu, J. D. Leng, Z. S. Meng, P. Vrabel, M. Orendac and M. L. Tong, *Chem. Commun.*, 2012, **48**, 12219.
4. F. S. Guo, J. D. Leng, J. L. Liu, Z. S. Meng and M. L. Tong, *Inorg. Chem.*, 2012, **51**, 405.
5. L. X. Chang, G. Xiong, L. Wang, P. Cheng and B. Zhao, *Chem. Commun.*, 2013, **49**, 1055.
6. G. Lorusso, M. A. Palacios, G. S. Nichol, E. K. Brechin, O. Roubeau and M. Evangelisti, *Chem. Commun.*, 2012, **48**, 7592.
7. M. Evangelisti, O. Roubeau, E. Palacios, A. Camon, T. N. Hooper, E. K. Brechin and J. J. Alonso, *Angew. Chem. Int. Ed.*, 2011, **50**, 6736.
8. J. B. Peng, Q. C. Zhang, X. J. Kong, Y. Z. Zheng, Y. P. Ren, L. S. Long, R. B. Huang, L. S. Zheng and Z. P. Zheng, *J. Am. Chem. Soc.*, 2012, **134**, 3314.
9. J. B. Peng, Q. C. Zhang, X. J. Kong, Y. P. Ren, L. S. Long, R. B. Huang, L. S. Zheng and Z. P. Zheng, *Angew. Chem. Int. Ed.*, 2011, **50**, 10649.
10. Y.-C. Chen, F.-S. Guo, Y.-Z. Zheng, J.-L. Liu, J.-D. Leng, R. Tarasenko, M. Orendac, J. Prokleška, V. Sechovský and M.-L. Tong, *Chem.–Eur. J.*, 2013, **19**, 13504.
11. R. Sibille, T. Mazet, B. Malaman and M. Franois, *Chem. Eur. J.*, 2012, **41**, 12970.
12. S. Biswas, A. Adhikary, S. Goswami and S. Konar, *Dalton Trans.*, 2013, **42**, 13331.
13. Y.-L. Hou, G. Xiong, P.-F. Shi, R.-R. Cheng, J.-Z. Cui and B. Zhao, *Chem. Commun.*, 2013, **49**, 6066.



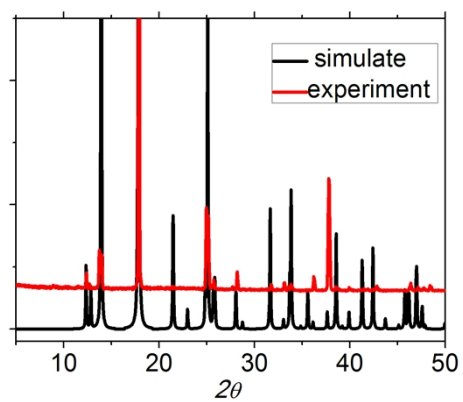
Scheme S1. The magnetic orbital interactions in $[M(\text{HCOO})_6]^{3-}\text{-Mn}^{\text{II}}$ ($M = \text{Fe}^{\text{III}}, \text{Cr}^{\text{III}}$) complexes.



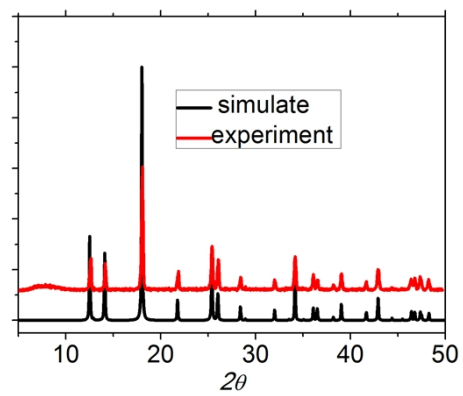
(a)



(b)



(c)



(d)

Fig. S1 The XRPD patterns of complexes **1** (a), **2** (b), **3** (c) and **4** (d).

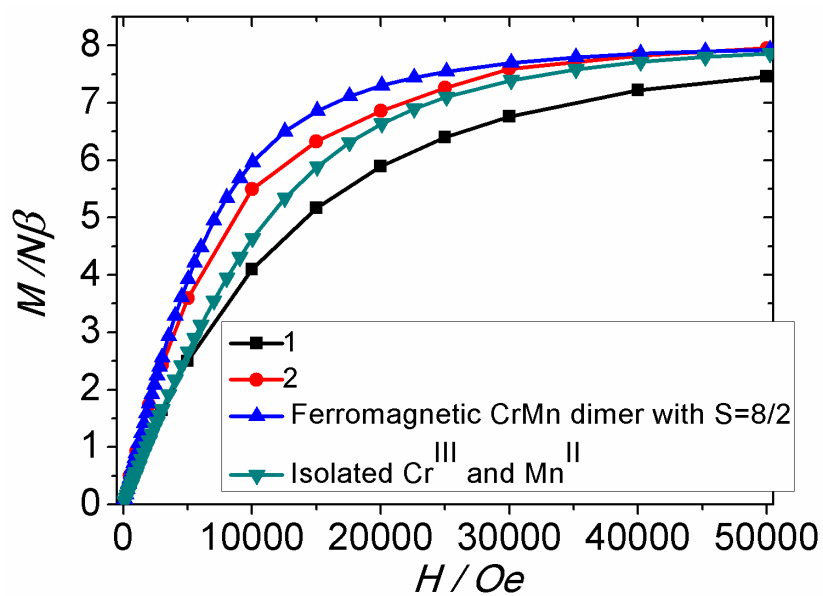
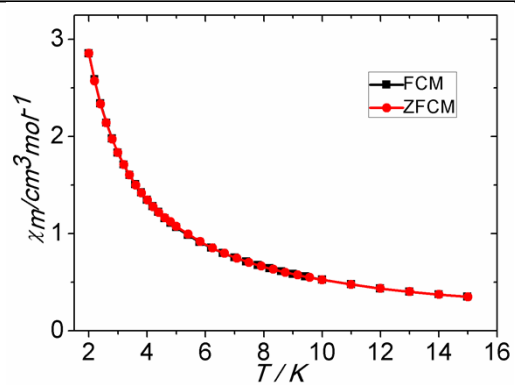
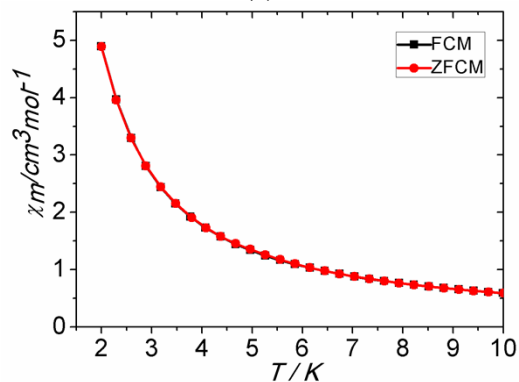


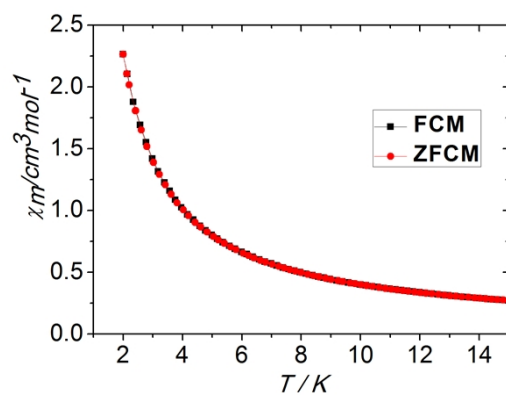
Fig. S2 $M/N\mu_B$ vs H plots of **1** and **2** at 2 K as well as the Brillouin function of ferromagnetic Cr^{III} - Mn^{III} dimer with $S = 8/2$ and two isolated high spin Cr^{III} and Mn^{II} with $g = 2.0$.



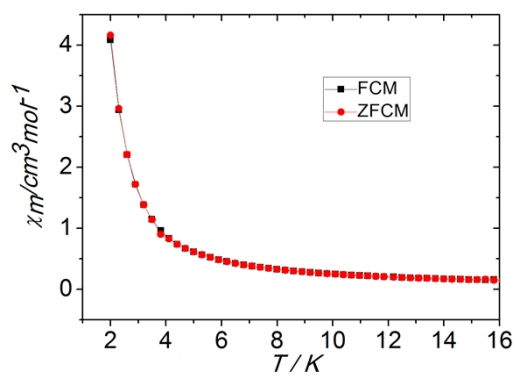
(a)



(b)



(c)



(d)

Fig. S3 ZFCM and FCM plots with external field of 50 Oe for **1** (a), **2** (b), **3**(c), and **4**(d) at low temperature.

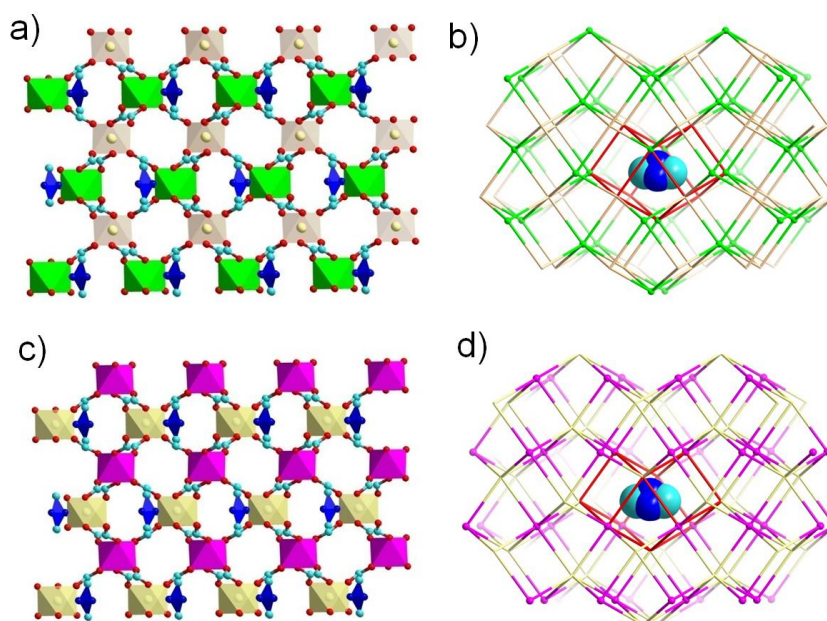


Fig. S4 (a) and (c) The polyhedron view of two sublattices of **3** and **4** with the cations filling in the cavities. (b) and (d) The Niccolite structural topology of **3** and **4** with the two sublattices. Mn^{II} in dark green, Cr^{III} in purple, Al^{III} and Mg^{II} in light yellow, O in red, N in blue and the H atoms omitted for clarity.

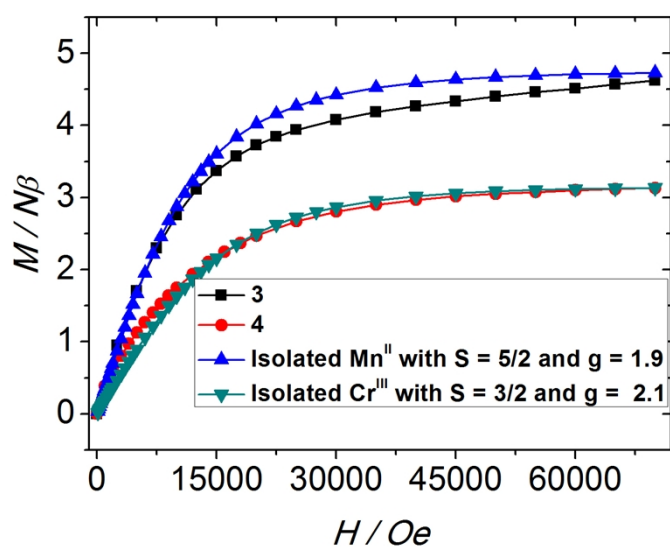


Fig. S5 $M/N \mu_B$ vs H plots of **2** and **3** at 2 K as well as the Brillouin function of isolated high spin ions Cr^{III} and Mn^{II} with $g = 2.0$.